Temperature-independent shear viscosity in a multiphase transport model for relativistic heavy ion collisions

Yao Zhang,[1,*] Jingbo Zhang,[2] Tong Chen,[1] Desheng Liu,[1] and Yun Chao[1]

[1]*School of Energy and Mechanical Engineering, Jiangxi University of Science and Technology, Nanchang 330013, China*

[2]*Department of Physics, Harbin Institute of Technology, Harbin 150001, China*

(Received 9 July 2017; revised manuscript received 15 August 2017; published 25 October 2017)

Using a multiphase transport (AMPT) model, we study the dependence on the specific shear viscosity of the transverse momentum spectra, Hanbury Brown–Twiss parameters, and elliptic flow with a temperature-independent shear viscous approach. The shear viscosity strengthens the transverse pressure gradients, raises the transverse momentum spectra, and gives smaller values of R_o, R_l, and R_o/R_s, but increases value of R_s. The transverse momentum dependence of v_2 is suppressed with increasing η/s and can hold at finite η/s within a partonic cascade approach in the AMPT model.

DOI: 10.1103/PhysRevC.96.044914

I. INTRODUCTION

The main goal of ultrarelativistic heavy-ion collisions is to understand collectivity in the strong interaction sector of the standard model and determine the transport properties of the quark-gluon plasma (QGP). Experiments at the BNL Relativistic Heavy-Ion Collider (RHIC) and the CERN Large Hadron Collider (LHC) have created the quark-gluon plasma and demonstrated that the QGP is strongly coupled and behaves as an almost perfect liquid with very small viscosity [1–4]. The specific shear viscosity η/s of QGP, which accelerates the transverse expansion, is important to the strongly interacting mediums viscous properties and transport evolution [5–7]. At finite temperature and zero chemical potential, the shear viscosity to entropy density ratio of QGP approaches the Kovtun-Starinets-Son (KSS) bound, $\eta/s \geqslant \frac{1}{4\pi}$, based on the anti–de Sitter/conformal field theory (AdS/CFT) correspondence [8]. Results from lattice QCD indicates that η/s is approximately temperature-independent at RHIC energy [9]. The ratio of η/s is evaluated in the range $\frac{1}{4\pi} \leqslant \eta/s \leqslant \frac{2.5}{4\pi}$ by a hybrid model which couples the viscous fluid dynamics to the ultrarelativistic quantum molecular dynamics (UrQMD) model via a Monte Carlo interface [10]. The values are $\eta/s = 0.12$ at RHIC and 0.2 at LHC via CGC saturation model with a prethermal classical evolution of the glasma gluon fields [11]. The specific shear viscosity is an important quantity to evaluate the strongly coupled nature of the QGP and pinpoint the location of the QGP phase transition which occurs in the vicinity of the minimum in η/s [12–14].

A significant effect of the finite η/s around the lower bound is shown within viscous hydrodynamics or cascade approaches [5,7,15–20]. Most hydrodynamical simulations assume a temperature-independent η/s, in order to describe elliptic flow data which cannot be larger than 2.5 times the lower KSS bound. The specific shear viscosity depends on the temperature and increases in the high-temperature QGP. The quantitative control of the temperature-independent η/s within a multiphase transport (AMPT) model can be used to study the effect of the finite η/s based on a partonic cascade approach which is different from the hydrodynamical simulations. The approximate control approach of the temperature-independent η/s in the AMPT model is also appropriate for the temperature-dependent η/s at high-temperature and convenient for setting arbitrary functional form of $\eta/s(T)$ at LHC energy. According to perturbative and lattice QCD, the temperature dependence of η/s is weak over the range explored in heavy-ion collisions at RHIC energy [21,22]. This suggests constant η/s can be approximately used at RHIC energy.

The AMPT model contains the evolution of partonic phase within a partonic cascade approach modeled by the Zhang's parton cascade (ZPC) model and provides a convenient way to study the specific shear viscosity of QGP. Based on the kinetic theory, the temperature dependence of η/s can be estimated by the QCD coupling constant α_s and the screening mass μ [23,24]. Using the screening mass depended on T, the effect of a constant (temperature-independent) ratio η/s can be studied in the transport theory. In previous work [25], we have studied the effect of approximate constant η/s on the HBT parameters in the string melting version of AMPT model with a rough assumption that the medium effect of the partonic phase at proper time is only related to the property of central medium and the spatial location effect is neglected. The rough assumption, which only evaluates the temperature and considers the effective average of η/s in a central cell, transverse radius $r_T < 2$ fm and space-time rapidity $|\eta_s| < 0.25$, overestimates the value of energy density away from the center and only can be used to study the effects of the shear viscosity on the observables qualitatively. The absence of the spatial anisotropy for the energy density distribution makes the assumption inappropriate for describing noncentral collisions or extracting η/s from the elliptic flow quantitatively.

In this paper, temperature-independent η/s contains the spatial location influence on the medium in the AMPT model with a Gaussian smearing. The screening mass is rearranged according to the energy density distribution calculated via describing parton by a three-dimensional Gaussian distribution of its total energy. In Sec. II, we consider a constant specific shear viscous approach in the AMPT model. In Sec. III, the

*yaozhang@jxust.edu.cn

transverse momentum spectra, Hanbury Brown–Twiss (HBT) radii and elliptic flow are discussed. We conclude in Sec. IV.

II. THE SPECIFIC SHEAR VISCOSITY IN THE AMPT MODEL

In kinetic theory the shear viscosity can be expressed as [26]

$$\eta = \frac{4\langle p\rangle}{15\sigma_{\rm tr}}, \tag{1}$$

where $\langle p\rangle$ is the mean momentum of partons and $\sigma_{\rm tr}$ is the transport cross section, defined by

$$\sigma_{\rm tr} = \int dt \frac{d\sigma}{dt} \sin^2\theta. \tag{2}$$

The AMPT model is a hybrid model which contains partonic and hadronic transport processes based on nonequilibration transport dynamics [27]. The process of partonic cascade included only two-body scatterings is calculated by the ZPC model with the differential scattering cross section [28]

$$\frac{d\sigma}{dt} \approx \frac{9\pi\alpha_s^2}{2(t-\mu^2)^2} \tag{3}$$

with t the standard Mandelstam variable. The partonic elastic scattering cross section is $\sigma_p \approx 9\pi\alpha_s^2/(2\mu^2)$. Using the differential scattering cross section, the transport cross section is given from Ref. [24] as

$$\sigma_{\rm tr} = \frac{18\pi\alpha_s^2}{E^2}\left[\left(1+\frac{2\mu^2}{E^2}\right)\ln\left(\frac{1+\mu^2/E^2}{\mu^2/E^2}\right)-2\right], \tag{4}$$

where E is the center of mass energy of the colliding parton pair. By assuming quark-gluon plasma of massless quarks at temperature T, the mean momentum is $\langle p\rangle = 3T$, the parton pair energy is $E \sim \sqrt{18}T$, and the energy density is $\epsilon = 12(4+3N_f)T^4/\pi^2 = 15.8T^4$ when using Boltzmann distributions with $N_f = 3$, where N_f is the number of relevant quark flavors, if only up, down, and strange quarks are considered [29]. The entropy density is $s = (\epsilon + P)/T = 4\epsilon/(3T)$. The shear viscosity to entropy density ratio is

$$\eta/s \approx \frac{27}{79\pi\alpha_s^2}\frac{1}{\left(9+\frac{\mu^2}{T^2}\right)\ln\left(\frac{18+\mu^2/T^2}{\mu^2/T^2}\right)-18}. \tag{5}$$

Thus, for fixed value of α_s, the screening mass depended on temperature, $\mu = cT$, leads to a temperature-independent ratio η/s. The ratio is related to the value of c and the constant ratios, $\eta/s = 0.08, 0.16$, and 0.24, are corresponding to the c value of 1.59, 2.37, and 2.82 with $\alpha_s = 0.47$. The screening mass of medium at coordinates (x,y,z) and time t can be approximately related to the energy density as follows:

$$\mu(x,y,z,t) = cT(x,y,z,t) = c\left[\frac{\epsilon(x,y,z,t)}{15.8}\right]^{\frac{1}{4}}. \tag{6}$$

At evolution time t of the partonic phase within the ZPC model, each pointlike parton is smeared with a three-dimensional Gaussian distribution of its total energy and the distribution function of energy density is given as [30,31]

$$\epsilon(x,y,z) = \sum N_i \exp\left[-\frac{(x-x_i)^2+(y-y_i)^2+(z-z_i)^2}{2\sigma^2}\right], \tag{7}$$

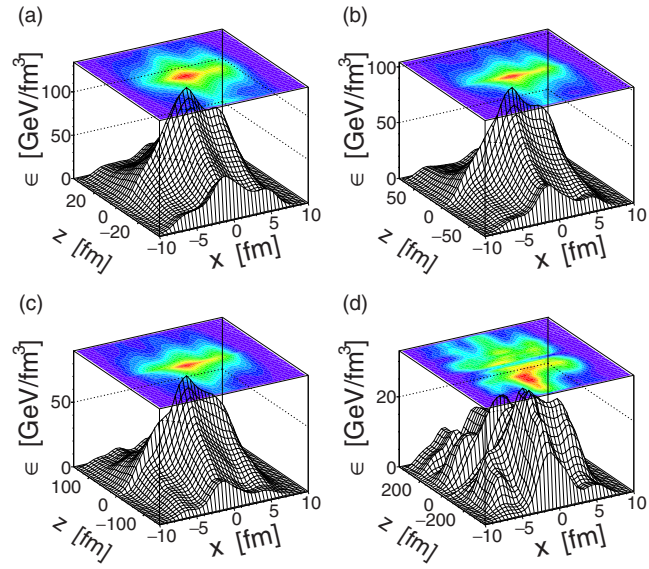

FIG. 1. Partonic energy density distribution in z-x plane for Au+Au central collisions at $\sqrt{s_{NN}} = 200$ GeV in the AMPT model: (a)–(d) correspond to $t = 0.5, 1.0, 2.0, 5.0$ fm/c.

where $N_i = (\frac{1}{2\pi})^{\frac{3}{2}}\frac{1}{\sigma^3}E_i$ provides the proper normalization, (x_i, y_i, z_i) and E_i are the position vector and energy of parton i. The Gaussian width is set at $\sigma = 0.5$ fm. Larger (smaller) value of σ leads to smaller (larger) fluctuations and hence reduced (enhanced) numerical instabilities.

Figures 1 and 2 show the partonic energy density distribution in the z-x and x-y plane, calculated in the AMPT model, for Au+Au collisions at $\sqrt{s_{NN}} = 200$ GeV in a central event with impact parameter $b = 0$ fm, where z is the beam axis and x is the in-plane axis. The distribution is azimuthally anisotropic and smooth stable, which indicates the calculated energy densities contain the spatial dependence and fluctuations. The

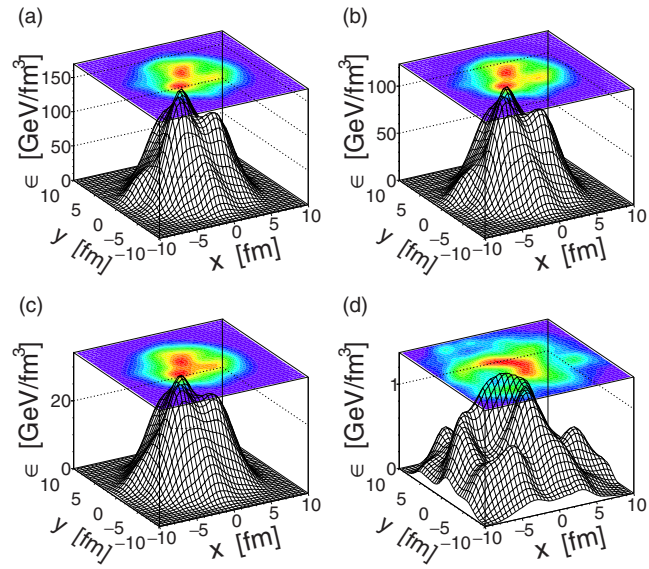

FIG. 2. Same as Fig. 1 but in x-y plane.

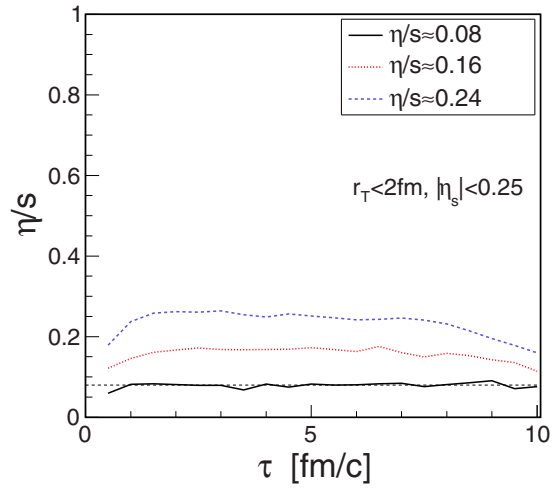

FIG. 3. Proper time evolution of shear viscosity to entropy density ratio for partonic phase.

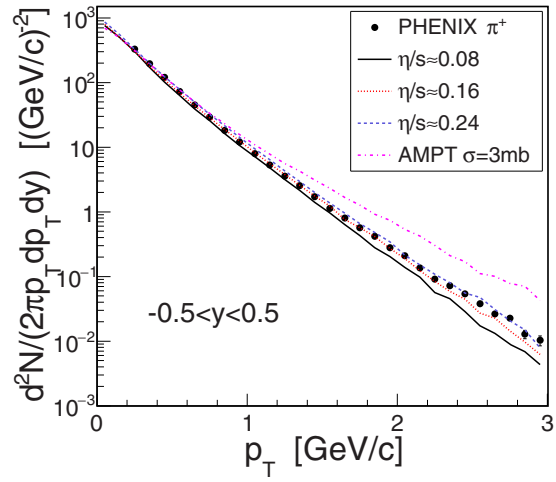

FIG. 4. The transverse momentum spectra of midrapidity pions for Au+Au central collisions at $\sqrt{s_{NN}} = 200$ GeV. PHENIX data from Ref. [34].

time evolution of partonic energy density is consistent with expectations that the energy density is highest in the center at early stage and becomes increasingly dispersed.

In order to check the approximate results of η/s, we calculate the energy-momentum tenser $T^{\mu\nu}$ by averaging over events in a volume V [32],

$$T^{\mu\nu} = \frac{1}{V}\sum_i \frac{p_i^\mu p_i^\nu}{E_i}, \tag{8}$$

where p_i^μ and E_i are the four-momentum and energy of particle i in the central cell and specifically, the longitudinal momentum p_z' in the local rest frame needs to be calculated from energy E and momentum p_z by $p_z' = (tp_z - zE)/\tau$. For the dissipative hydrodynamics in the boost-invariant Bjorken expansion, the ratio η/s can be calculated [5,9,33],

$$\eta = \frac{\tau}{4}(T^{11} + T^{22} - 2T^{33}), \tag{9}$$

and $s \approx 4n$, where n is the number density of partons. The AMPT model is not satisfied with the Bjorken expansion, but the medium in the central cell is approximate satisfied with the boost-invariant and the shear viscosity is appropriately estimated by Eq. (9).

Figure 3 shows the proper time evolution of the specific shear viscous ratio in the central cell for Au+Au central collisions at $\sqrt{s_{NN}} = 200$ GeV. The calculated ratios η/s are close to the expected constant ratio. The curves of η/s has a slow drop which is more obvious with larger η/s after 5 fm/c. The drop of curve with large shear viscosity is due to the η/s calculation in Eq. (9) which assume a one-dimensional Bjorken expansion. The boost-invariant character is satisfied when partons are close to the center. We calculate η/s in a particular central cell and the longitudinal size and cell volume increase with time evolution. The shear viscosity accelerates the transverse expansion and restrains the longitudinal expansion. The longitudinal restrain increases the deviate from the boost-invariant expansion with increasing longitudinal size and leads to the drop of η/s at large proper time.

III. TRANSVERSE MOMENTUM SPECTRA, HBT RADII, AND ELLIPTIC FLOW

The default Lund string fragmentation parameters in the HIJING model, $a = 0.5$ and $b = 0.9\,\mathrm{GeV}^{-2}$, work well for $p + p$ collisions. The parameters, $a = 2.2$ and $b = 0.5\,\mathrm{GeV}^{-2}$, in the default version of the AMPT model are used in order to fit the charged particle yield in Pb+Pb collisions at CERN Super Proton Synchrotron (SPS). For heavy-ion collisions at RHIC energies, the AMPT model with default parameters overestimates the charged particle yield while underestimates the slopes of the transverse momentum spectra. In Ref. [29], setting the values of the Lund string fragmentation parameters to $a = 0.55$ and $b = 0.15\,\mathrm{GeV}^{-2}$ at RHIC energy enable the results of the transverse momentum spectra and elliptic flow to fit the experimental data. The parameters are used in the AMPT model with $\alpha_s = 0.33$ in this paper.

Figure 4 shows the transverse momentum spectra of pions at midrapidity compared with PHENIX data from central Au+Au collisions at $\sqrt{s_{NN}} = 200$ GeV. The transverse momentum spectra result with $\eta/s = 0.16$ is close to the experimental data. It can be seen that η/s has significant effect on the transverse momentum spectra. The shear viscosity raises the transverse momentum spectra of pions. The reason is that larger shear viscosity strengthens the transverse pressure gradients and leads to larger radial flow.

The HBT correlation function, which is calculated by the correlation after burner (CRAB) program without the final state interactions, can be fitted by the Bertsch-Pratt parametrization in the 'out-side-long' coordinate system [35,36],

$$C(\mathbf{q}) = 1 + \lambda \exp\left(-q_o^2 R_o^2 - q_s^2 R_s^2 - q_l^2 R_l^2\right), \tag{10}$$

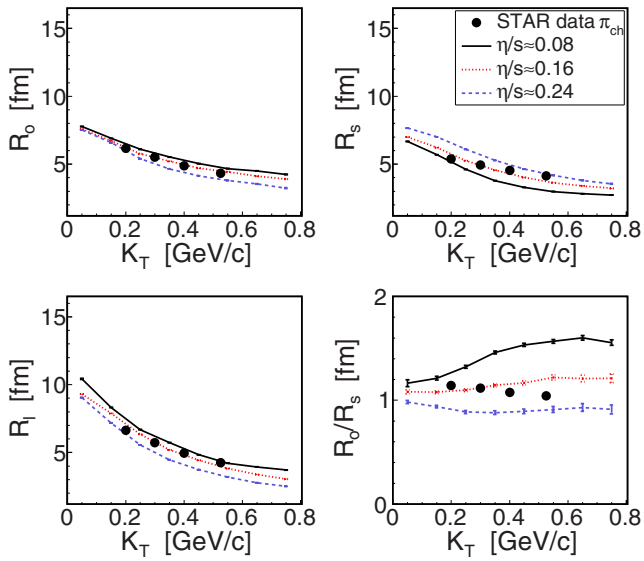

FIG. 5. Two-pion HBT radii R_o, R_s, R_l and the ratio R_o/R_s for Au+Au central collisions at $\sqrt{s_{NN}} = 200$ GeV. STAR data from Ref. [37].

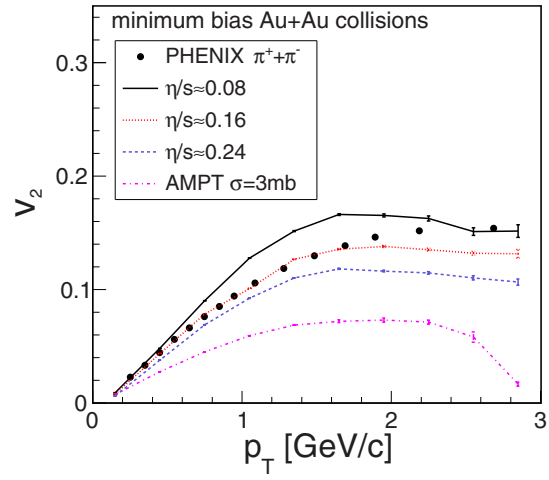

FIG. 6. The dependence of the differential elliptic flow v_2 on η/s for charged pions obtained in minimum-bias Au+Au collisions at $\sqrt{s_{NN}} = 200$ GeV. PHENIX data from Ref. [38].

where q_o, q_s, q_l are three components of the relative momentum difference $\mathbf{q} = \mathbf{p_1} - \mathbf{p_2}$ of a pair of pions. Fitting the correlation function can obtain size parameters R_o, R_s, and R_l which are so-called HBT radii.

Figure 5 shows the HBT radii R_o, R_s, R_l and the ratio R_o/R_s as a function of average transverse momentum K_T in Au+Au central collisions at $\sqrt{s_{NN}} = 200$ GeV. η/s reduces the values of radii R_o and R_l, but increases value of R_s. Thus, η/s gives smaller values of R_o/R_s, which has similar results with the viscous hydrodynamic prediction and indicates that the shear viscosity accelerates the transverse expansion.

Elliptic flow is defined as one half of the second Fourier coefficient of the particle transverse momentum distribution on the azimuthal angle and can be calculated as [39,40]

$$v_2 = \left\langle \frac{p_x^2 - p_y^2}{p_x^2 + p_y^2} \right\rangle, \tag{11}$$

where $\langle \cdots \rangle$ indicates an average over all particles in all events.

Figure 6 shows the dependence of the differential elliptic flow v_2 on η/s for charged pions obtained in minimum-bias Au+Au collisions at $\sqrt{s_{NN}} = 200$ GeV. Different values of η/s lead to a significantly difference of v_2 and change its transverse momentum dependence. Larger specific shear viscosity leads to a stronger suppression of v_2 which is due to the viscous suppression of anisotropic flow. The v_2 and transverse momentum spectra results suggest the average value of $\eta/s \sim 0.16$. v_2 is not only dependent on the transport properties of medium but also proportional to the initial spatial anisotropy of the collision region and affected by the temperature dependence of η/s [10,18,41,42]. These influences will be studied in a separate article.

In Ref. [25], we also estimated the shear viscosity by Eq. (9) and studied the effect of η/s on the observables with a rough assumption calculated the energy density in a central cell. In this paper, the estimated η/s with time evolution in Fig. 3 is close to our previous results, because the averaged energy densities in the region of the central cell are similar, which lead to similar effects of η/s on the system evolution. But it is obvious that the difference, between the energy density calculated by Eq. (7) and the averaged value in the central cell, increases with increasing distance from center in Figs. 1 and 2. The averaged energy density in the central cell overestimates the value of energy density away from the center, which leads to an overestimated specific shear viscosity and strengthens the transverse expansion, and does not contain the spatial anisotropy of the energy density distribution for noncentral collisions. The overestimated η/s unreasonably increases the transverse momentum spectra and suppresses the value of elliptic flow. It is reasonable to replace the averaged energy density with the distribution function of energy density.

The results of the transverse momentum spectra and the elliptic flow from the normal AMPT model, where η/s is not forced to be constant and the parton cross section $\sigma_p = 3$ mb is used, are shown in Figs. 4 and 6. The AMPT model naturally provides a temperature dependent η/s which decreases as the temperature increases for fixed values of σ_p and α_s. The usual intrinsic temperature dependent η/s of the AMPT model is inconsistent with the results of perturbative and lattice QCD. η/s of the normal AMPT model is close to the KSS bound at high-temperature and rises rapidly to 10 times the bound as the temperature drops to the critical temperature T_c. The unreasonable temperature dependent η/s significantly increases the transverse momentum spectra in Fig. 4 and suppresses the elliptic flow in Fig. 6. Compared with the temperature-independent shear viscous results, the transverse momentum spectra and the elliptic flow from the normal AMPT model deviate far from the experimental data.

IV. SUMMARY

Based on the AMPT model, we consider an approach of the temperature-independent shear viscosity with a Gaussian

smearing function and study the dependence on the specific shear viscosity of the pion transverse momentum spectra, HBT parameters, and differential elliptic flow for Au+Au collisions at RHIC energy $\sqrt{s_{NN}} = 200\,\mathrm{GeV}$. The shear viscosity strengthens the transverse pressure gradients and raises the transverse momentum spectra. η/s gives smaller values of R_o, R_l, and $R_\mathrm{o}/R_\mathrm{s}$, but increases value of R_s, which indicates that R_o and R_l are sensitive to the transverse and longitudinal expansion, respectively, and R_s is most related to the source size. The effect of the shear viscosity on the HBT radii and $R_\mathrm{o}/R_\mathrm{s}$ is gradually diminished with increasing η/s. For temperature-independent η/s, the suppression effects of the elliptic flow increase monotonically with shear viscosity. The results of v_2 are qualitative similar with viscous hydrodynamics and suggest the value of $\eta/s \sim 0.16$ which is close to the PHENIX data. The transverse momentum dependence of v_2 advocated as a signature of the perfect hydrodynamical behavior can hold at finite η/s within a partonic cascade approach in the AMPT model.

ACKNOWLEDGMENTS

This work was supported by the National Natural Science Foundation of China (NSFC Grant No. 11647148) and the Science and Technology Project of Jiangxi Provincial Education Department (China) (Grant No. GJJ160663).

[1] I. Arsene *et al.* (BRAHMS Collaboration), Nucl. Phys. A **757**, 1 (2005).
[2] B. B. Back *et al.* (PHOBOS Collaboration), Nucl. Phys. A **757**, 28 (2005).
[3] K. Adcox *et al.* (PHENIX Collaboration), Nucl. Phys. A **757**, 184 (2005).
[4] J. Adams *et al.* (STAR Collaboration), Nucl. Phys. A **757**, 102 (2005).
[5] D. Teaney, Phys. Rev. C **68**, 034913 (2003).
[6] S. Pratt and J. Vredevoogd, Phys. Rev. C **78**, 054906 (2008).
[7] S. Pratt, Phys. Rev. Lett. **102**, 232301 (2009).
[8] P. K. Kovtun, D. T. Son, and A. O. Starinets, Phys. Rev. Lett. **94**, 111601 (2005).
[9] N. Armesto *et al.*, J. Phys. G: Nucl. Part. Phys. **35**, 054001 (2008).
[10] H. Song, S. A. Bass, U. Heinz, T. Hirano, and C. Shen, Phys. Rev. Lett. **106**, 192301 (2011).
[11] C. Gale, S. Jeon, B. Schenke, P. Tribedy, and R. Venugopalan, Phys. Rev. Lett. **110**, 012302 (2013).
[12] L. P. Csernai, J. I. Kapusta, and L. D. McLerran, Phys. Rev. Lett. **97**, 152303 (2006).
[13] R. A. Lacey, N. N. Ajitanand, J. M. Alexander, P. Chung, W. G. Holzmann, M. Issah, A. Taranenko, P. Danielewicz, and H. Stöcker, Phys. Rev. Lett. **98**, 092301 (2007).
[14] R. A. Lacey, A. Taranenko, J. Jia, D. Reynolds, N. N. Ajitanand, J. M. Alexander, Y. Gu, and A. Mwai, Phys. Rev. Lett. **112**, 082302 (2014).
[15] C. Shen, U. Heinz, P. Huovinen, and H. Song, Phys. Rev. C **82**, 054904 (2010).
[16] H. Song, S. A. Bass, and U. Heinz, Phys. Rev. C **83**, 054912 (2011).
[17] H. Niemi, G. S. Denicol, P. Huovinen, E. Molnár, and D. H. Rischke, Phys. Rev. Lett. **106**, 212302 (2011).
[18] E. Molnár, H. Holopainen, P. Huovinen, and H. Niemi, Phys. Rev. C **90**, 044904 (2014).
[19] G. Ferini, M. Colonna *et al.*, Phys. Lett. B **670**, 325 (2009).
[20] A. Chaudhuri, Phys. Lett. B **713**, 91 (2012).
[21] P. Arnold, G. D. Moore, and L. G. Yaffe, J. High Energy Phys. 05 (2003) 051.
[22] A. Nakamura and S. Sakai, Phys. Rev. Lett. **94**, 072305 (2005).
[23] J. Xu and C. M. Ko, Phys. Rev. C **84**, 014903 (2011).
[24] J. Xu and C. M. Ko, Phys. Rev. C **83**, 034904 (2011).
[25] Y. Zhang, J. B. Zhang, J. L. Liu, and L. Huo, Phys. Rev. C **92**, 014909 (2015).
[26] M. H. Thoma, Phys. Rev. D **49**, 451 (1994).
[27] Z.-W. Lin, C. M. Ko, B.-A. Li, B. Zhang, and S. Pal, Phys. Rev. C **72**, 064901 (2005).
[28] B. Zhang, Comput. Phys. Commun. **109**, 193 (1998).
[29] Z. W. Lin, Phys. Rev. C **90**, 014904 (2014).
[30] J. Steinheimer, M. Bleicher, H. Petersen, S. Schramm, H. Stöcker, and D. Zschiesche, Phys. Rev. C **77**, 034901 (2008).
[31] L. G. Pang, Q. Wang, and X. N. Wang, Phys. Rev. C **86**, 024911 (2012).
[32] B. Zhang, L. W. Chen, and C. M. Ko, J. Phys. G: Nucl. Part. Phys. **35**, 065103 (2008).
[33] P. Danielewicz and M. Gyulassy, Phys. Rev. D **31**, 53 (1985).
[34] S. S. Adler *et al.* (PHENIX Collaboration), Phys. Rev. C **69**, 034909 (2004).
[35] S. Pratt *et al.*, Nucl. Phys. A **566**, 103 (1994).
[36] S. S. Adler *et al.* (PHENIX Collaboration), Phys. Rev. Lett. **93**, 152302 (2004).
[37] J. Adams *et al.* (STAR Collaboration), Phys. Rev. C **71**, 044906 (2005).
[38] A. Adare *et al.* (PHENIX Collaboration), Phys. Rev. Lett. **98**, 162301 (2007).
[39] A. M. Poskanzer and S. A. Voloshin, Phys. Rev. C **58**, 1671 (1998).
[40] S. S. Adler *et al.* (PHENIX Collaboration), Phys. Rev. Lett. **91**, 182301 (2003).
[41] R. Snellings, New J. Phys. **13**, 055008 (2011).
[42] H. Niemi, K. J. Eskola, and R. Paatelainen, Phys. Rev. C **93**, 024907 (2016).